1304 *Inorg. Chem.* **2010**, *49*, 1304–1306
DOI: 10.1021/ic902298y

Inorganic Chemistry
Communication

Large Spin-State Changes in Isostructural Cyanate- and Azide-Bridged $Mn_3^{III}Mn_2^{II}$ Single-Molecule Magnets

Patrick L. Feng,[†] Casey J. Stephenson,[†] Asma Amjad,[‡] Gavin Ogawa,[†] Enrique del Barco,[‡] and David N. Hendrickson*,[†]

[†]*Department of Chemistry and Biochemistry, University of California, San Diego, La Jolla, California 92093-0358 and* [‡]*Department of Physics, University of Central Florida, Orlando, Florida 32816-2385*

Received November 19, 2009

We prepared three structurally related $Mn_3^{III}Mn_2^{II}$ complexes that possess $S \approx 1-11$ spin ground states as a result of variations in the geometry and identity of μ_2-η^1:η^1 bridging groups. These complexes function as single-molecule magnets yet demonstrate other interesting behavior such as quasi-classical magnetization hysteresis and comparable magnetization reversal barriers (U_{eff}).

Quantum phenomena in single-molecule magnets (SMMs) have been observed for a large number of complexes over the past 15 years.[1] Numerous fascinating properties have been reported, including quantum tunneling of the magnetization (QTM),[2] quantum-phase interference,[3] exchange-biased QTM,[4] spin-parity effects,[5] and quantum coherence.[6] In spite of the large body of work documenting these behaviors, fundamental processes such as the mechanism for QTM are still not fully understood. The recently reported C_3-symmetric complex $[NEt_4]_3[Mn_3Zn_2(salox)_3O(N_3)_6Cl_2]$ (saloxH$_2$ = salicylaldoxime) represents the first example of a SMM that obeys the symmetry-dependent selection rules for QTM. This was manifested as the observation of QTM between spin states with $\Delta m_s = 3n$, in which n is an integer.[7,8] These studies also provided insight about the important roles of weak dipolar interactions and tilting of the single-ion Jahn−Teller axes upon the symmetry-forbidden QTM resonances, which is relevant to *all* SMMs.

We report here the structures and magnetic properties for three closely related $Mn_3^{III}Mn_2^{II}$ complexes that exhibit highly variable spin ground states. The ferromagnetically coupled $S = 11$ complex **1** is described by $[NEt_4]_3[Mn_5(salox)_3O(N_3)_6Br_2]$, as shown in Figure 1. The analogous $S = 6$ Me-salox^{2-} complex **2** retains a similar molecular structure and is described as $[NEt_4]_3[Mn_5(Me\text{-}salox)_3O(N_3)_6Cl_2]$. The antiferromagnetically coupled $S = 1$ complex **3** has the formula $[NEt_4]_3[Mn_5(salox)_3O(OCN)_6Cl_2]$ and differs from **1** and **2** in the identity of the μ_2-η^1:η^1 groups, where six OCN^- bridges replace the corresponding azides. All of these complexes crystallize in the trigonal space group $R3c$ with very similar unit cell parameters.

On the basis of previous magnetostructural studies on $Mn_3^{III}Zn_2^{II}$ analogues, these complexes each possess a ferromagnetic $S = 6$ Mn_3^{III} core structure, with the overall spin ground state being determined by the μ_2-η^1:η^1-azide bridging geometry in **1** and **2** and the switch to cyanate-mediated antiferromagnetic interactions in **3**. In view of the highly variable spin ground states and similar projections of the single-ion zero-field-splitting anisotropies onto the molecular easy axis, one would anticipate these molecules to exhibit significantly different magnetization reversal barriers, estimated as $\Delta E \approx |D| \cdot S_z^2$. This was surprisingly not the case for **1**−**3**, in which very similar U_{eff} values ranging from 33.9 to 39.4 K were observed.

Table 1 summarizes the structural parameters for complexes **1**−**3**, in which subtle differences are apparent. The $Mn^{III}-N-O-Mn^{III}$ torsion angle (θ) has been shown to correlate with the magnetic exchange interactions between Mn^{III} ions, where torsion angles of $\theta \geq 31°$ result in larger ferromagnetic exchange parameters.[8,10−12] On the basis of

*To whom correspondence should be addressed. E-mail: dhendrickson@ucsd.edu. Fax: 858-534-5383.

(1) Gatteschi, D.; Sessoli, R.; Villain, J. *Molecular Nanomagnets*; Oxford Publishing: New York, 2006.
(2) Gatteschi, D.; Caneschi, A.; Pardi, L.; Sessoli, R. *Science* **1994**, *265*, 1054.
(3) Ramsey, C. M.; del Barco, E.; Hill, S.; Shah, S.; Beedle, C. C.; Hendrickson, D. N. *Nat. Phys.* **2008**, *4*, 277.
(4) Wernsdorfer, W.; Sessoli, R. *Science* **1999**, *284*, 133.
(5) Wernsdorfer, W.; Bhaduri, S.; Tiron, R.; Hendrickson, D. N.; Christou, G. *Phys. Rev. Lett.* **2002**, *89*, 197201.
(6) Takahashi, S.; van Tol, J.; Beedle, C. C.; Hendrickson, D. N.; Brunel, L.-C.; Sherwin, M. S. *Phys. Rev. Lett.* **2009**, *102*, 087603.
(7) Henderson, J. J.; Koo, C.; Feng, P. L.; del Barco, E.; Hill, S.; Tupitsyn, I. S.; Stamp, P. C. E.; Hendrickson, D. N. *Phys. Rev. Lett.* **2009**, *103*, 017202.
(8) Feng, P. L.; Koo, C.; Henderson, J. J.; Manning, P.; Nakano, M.; del Barco, E.; Hill, S.; Hendrickson, D. N. *Inorg. Chem.* **2009**, *48*, 3480.
(9) Yang, C.-I.; Wernsdorfer, W.; Lee, G.-H.; Tsai, H.-L. *J. Am. Chem. Soc.* **2007**, *129*, 456.
(10) Milios, C.; Vinslava, A.; Wernsdorfer, W.; Prescimone, A.; Wood, P. A.; Parsons, S.; Perlepes, S. P.; Christou, G.; Brechin, E. K. *J. Am. Chem. Soc.* **2007**, *129*, 6547.
(11) Inglis, R.; Jones, L. F.; Karotsis, G.; Collins, A.; Parsons, S.; Perlepes, S. P.; Wernsdorfer, W.; Brechin, E. K. *Chem. Commun.* **2008**, 5924.
(12) Inglis, R.; Jones, L. F.; Mason, K.; Collins, A.; Moggach, S. A.; Parsons, S.; Perlepes, S. P.; Wernsdorfer, W.; Brechin, E. K. *Chem.—Eur. J.* **2008**, *14*, 9117.

 Published on Web 01/19/2010 © 2010 American Chemical Society

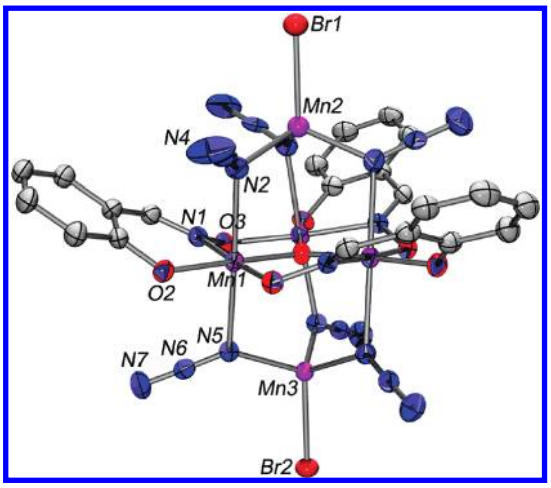

Figure 1. ORTEP for complex **1** at the 50% probability level. Carbon and symmetry-equivalent atoms have been left unlabeled for clarity.

Table 1. Selected Structural Parameters for Complexes **1**−**3**

	1	**2**	**3**
θ (deg)	33.58(2)	37.07(3)	31.93(2)
ε_{upper} (deg)	109.89(1)	105.50(2)	108.23(3)
ε_{lower} (deg)	108.25(1)	112.30(1)	105.27(3)
Mn^{III}−Mn^{III} (Å)	3.286(3)	3.283(2)	3.284(2)
Mn^{III}−Mn^{II}_{upper} (Å)	3.588(3)	3.546(3)	3.627(2)
Mn^{III}−Mn^{II}_{lower} (Å)	3.573(4)	3.693(2)	3.560(2)

these results, complexes **1**−**3** are all expected to exhibit ferromagnetic Mn^{III}−Mn^{III} interactions, with the strongest and weakest exchanges occurring in **2** and **3**, respectively. Less understood are the structural and magnetic relationships for azide- and cyanate-bridged Mn^{III}−Mn^{II} interactions, in which no systematic study of these exchange pathways has been reported. The Mn^{III}−N−Mn^{II} bridging angles (ε) for **1**−**3** range from 105.27° to 112.30°, resulting in a stepwise change from entirely ferromagnetic interactions in **1** [$S = (6 + {}^5/_2 + {}^5/_2) = 11$] to a balance of ferromagnetic and antiferromagnetic interactions in **2** [$S = (6 + {}^5/_2 - {}^5/_2) = 6$] to fully antiferromagnetic interactions in **3** [$S = (6 - {}^5/_2 - {}^5/_2) = 1$] (vide infra). This is due to changes in the ε angles in **1** and **2** and the switch to cyanate bridges in **3**. It is notable that the differences observed here are distinct from those in prior studies on oximate-bridged Mn^{III}-based SMMs, in which the emphasis was formerly placed upon the bonding geometry of the oximate groups relative to the Mn^{III} ions.[8,10−12]

Direct-current (dc) susceptibility measurements were collected at 0.1 T from 1.8 to 300 K to assess the nature of magnetic exchange in **1**−**3**, as shown in Figure 2. Complex **1** exhibits the largest $\chi_M T$ value of 52.7 $cm^3 \cdot K \cdot mol^{-1}$ at 2.81 K, which compares to the value of 55.0 $cm^3 \cdot K \cdot mol^{-1}$ expected for an $S = 10$ system with $g = 2.0$. The susceptibility data for **2** suggest a lower spin ground state, where the maximum $\chi_M T$ value of 31.9 $cm^3 \cdot K \cdot mol^{-1}$ at 20 K is slightly larger than the value of 28.0 $cm^3 \cdot K \cdot mol^{-1}$ expected for an $S = 7$ complex. The susceptibility data for **3** reveal a 1.8 K $\chi_M T$ value of 1.1 $cm^3 \cdot K \cdot mol^{-1}$, which compares closely with the value of 1.0 $cm^3 \cdot K \cdot mol^{-1}$ expected for an $S = 1$ system. Unfortunately, it was not possible to reliably fit these data in the absence of full-matrix diagonalization techniques employing an uncoupled basis set. These results will be reported in a future work because of the complexity of applying this procedure to these complexes.

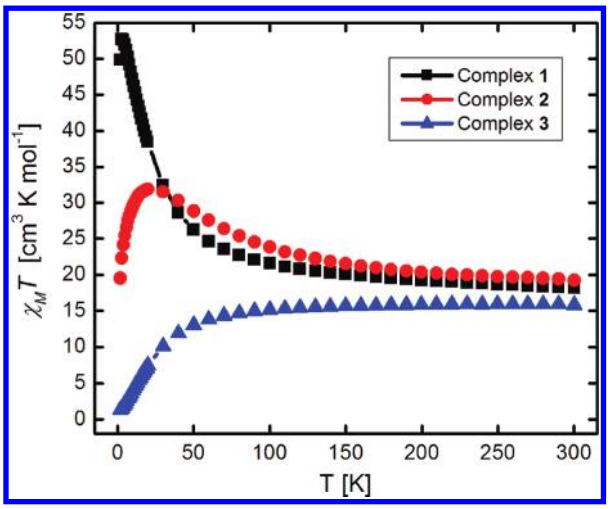

Figure 2. Plot of the 0.1 T $\chi_M T$ data for complexes **1**−**3** from 300 to 1.8 K. Solid lines serve as guides for the eye.

$$H = D\hat{S}_z^2 + g\mu_B\mu_0\hat{S}_z H_z \quad (1)$$

Variable-field reduced magnetization data were collected on complexes **1**−**3** from 1 to 5 T and fit to the Hamiltonian described by eq 1. The least-squares fitting results for complex **1** indicate an $S = 10$ spin ground state with fitting parameters of $g = 1.91$ and $D = -0.29$ K. An analogous fit for complex **2** indicates an $S = 6$ spin ground state and fitting parameters of $g = 1.84$ and $D = -0.86$ K, revealing a much smaller spin and significantly larger anisotropy than those in **1**. Interestingly, these parameters lead to similarly calculated thermodynamic barriers of 29 and 31 K for **1** and **2**, respectively. It was not possible to fit the reduced magnetization data of **3** to the Hamiltonian shown above, suggesting a significant degree of excited-state spin mixing into the ground state.

Alternating-current (ac) susceptibility data were collected on complexes **1**−**3** at 10−1000 Hz from 7.0 to 1.8 K, revealing clear peaks in the out-of-phase susceptibility (χ''_M) along with corresponding decreases in the in-phase susceptibility (χ'_M) (Figures 3 and S7 and S9 in the Supporting Information). Extrapolation of the in-phase susceptibility product ($\chi'_M T$) to 0 K was performed for **1**−**3**, providing verification of the spin ground states in the absence of an applied field. These extrapolation results indicate $S = 11$, 6, and 1 ground states for **1**−**3**, respectively. Arrhenius plots were constructed from the out-of-phase ac susceptibility data for each complex (Figures S6, S8, and S10 in the Supporting Information), resulting in effective magnetization reversal barriers (U_{eff}) of 36.4, 39.4, and 33.9 K for **1**−**3**, respectively. These values are peculiarly larger than the predicted thermodynamic barriers obtained from fits to the reduced magnetization data. This implies possible oversimplifications of the Hamiltonian given in eq 1, with the most probable cause being the assumption of a perfectly isolated ground state. This is supported by the $S \pm 1$ variation for the ground states indicated by the dc and ac susceptibility data, which is suggestive of the thermal population of low-lying excited spin states below 7 K. The sharp increase in χ''_M below 2.2 K for complex **3** provides further evidence for a complicated relaxation process, as is evident in

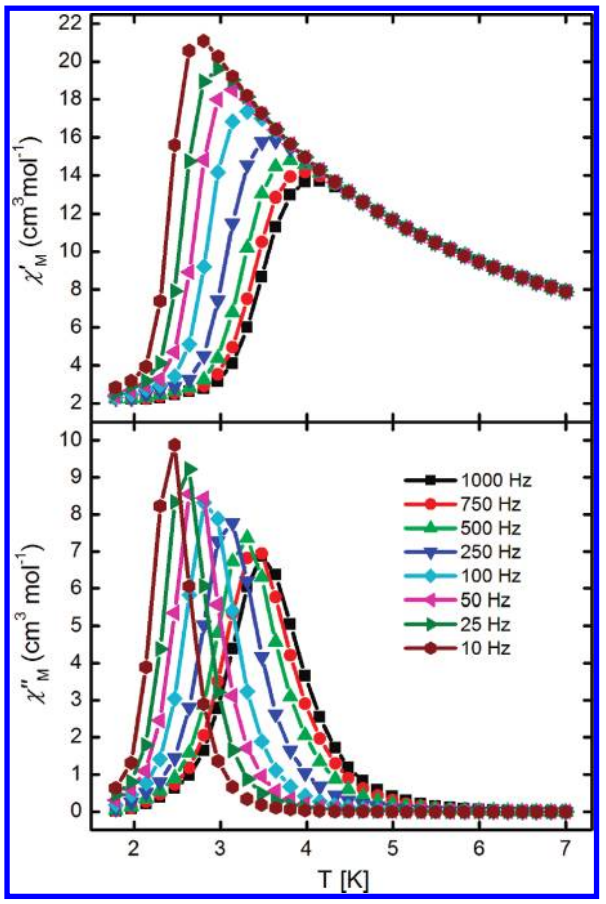

Figure 3. Plots of the in-phase susceptibility (χ'_M; top) and out-of-phase susceptibility (χ''_M; bottom) for complex **1** from 1.8 to 7.0 K at the frequencies indicated.

Figure S9 in the Supporting Information. Nonetheless, it is remarkable that U_{eff} is larger in complex **2** than in **1**, despite its much smaller ground-state spin value and close structural similarities. The appreciable U_{eff} value of 33.9 K for **3** is another notable observation considering the exceedingly small $S = 1$ ground state.

Single-crystal magnetization hysteresis measurements were conducted on complex **1**, with the field applied along the easy axis of the molecule. The resulting hysteresis loops are shown in Figure 4 and are surprising considering the absence of vertical steps that are characteristic of QTM. This observation is even more interesting considering that both of the previously studied $[NEt_4]_3[Mn_5(salox)_3O(N_3)_6Cl_2]$ and $[NEt_4]_3[Mn_3Zn_2(salox)_3O(N_3)_6Cl_2]$ analogues exhibit QTM in the hysteresis loops, the latter of which possesses extremely clean and well-defined QTM resonances that are among the sharpest observed for any SMM.[7,9] Because **1** is isostructural and crystallographically isomorphic to $[NEt_4]_3[Mn_3Zn_2(salox)_3O(N_3)_6Cl_2]$, the explanation behind the absence of QTM resonances in **1** likely stems from the weak exchange interaction between Mn^{II} and Mn^{III} ions, as is qualitatively evident from the increase in $\chi_M T$ at only low temperatures. Importantly, in the absence of QTM steps,

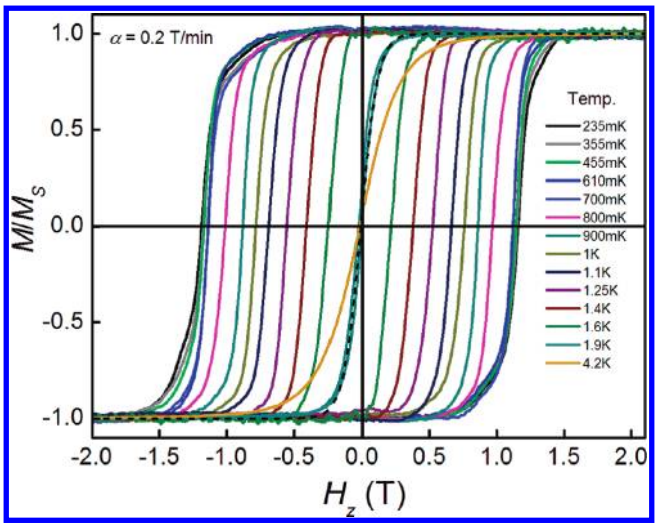

Figure 4. Hysteresis measurements for a single crystal of **1** from 0.235 to 4.2 K, at a sweep rate of 0.2 T·min^{-1}. The magnetization is normalized by the saturation value M_s.

temperature-independent tunneling is still indicated below 800 mK as a plateau in a plot of the coercive field versus temperature, as shown in Figure S11 in the Supporting Information. Although more detailed experiments to understand this behavior in detail are in progress, the most likely explanation involves the presence of multiple low-lying excited states as a result of weak magnetic exchange interactions between the Mn ions in this complex. This may lead to a quasi-continuous distribution of spin states, resulting in hysteretic behavior that is reminiscent of a classical magnetic nanoparticle.

Thus, we report here three new $Mn_3^{III}Zn_2^{II}$ complexes that possess highly variable spin ground states and anisotropies as a result of changes in the $Mn^{III}-N-Mn^{II}$ bridging angles and the identity of the μ_2-η^1:η^1 bridging groups. Remarkably similar U_{eff} barriers were observed for complexes **1**−**3**, revealing an approximate inverse-square relationship between the spin (S) and molecular anisotropy (D) in **1** and **2** and the role of low-lying excited states in **3**. These observations provide insight toward the optimization of SMM properties in these complexes; i.e., it is not possible to independently vary S and D. In addition to this behavior, vertical steps corresponding to QTM are absent in the single-crystal hysteresis loops for **1**, suggesting the presence of an additional mechanism(s) for magnetization relaxation. Future work will include a more detailed analysis of these observations, as well as the extension of these results to other SMM systems.

Acknowledgment. This work was supported by the National Science Foundation.

Supporting Information Available: Crystallographic information in CIF format and ac susceptibility data. This material is available free of charge via the Internet at http://pubs.acs.org.